Journal of Nuclear Materials 385 (2009) 223–227

Contents lists available at ScienceDirect

Journal of Nuclear Materials

journal homepage: www.elsevier.com/locate/jnucmat

An object Kinetic Monte Carlo Simulation of the dynamics of helium and point defects in tungsten

C.S. Becquart [a,*], C. Domain [a,b]

[a] Laboratoire de Métallurgie Physique et Génie des Matériaux, UMR 8517, Université de Lille 1, F-59655 Villeneuve d'Ascq cedex, France
[b] EDF-R&D Département MMC, Les Renardières, F-77818 Moret sur Loing cedex, France

ARTICLE INFO

PACS:
71.20.Be
71.15.Mb
61.72.J–

ABSTRACT

In the near surface of plasma facing materials, high concentrations of hydrogen and helium isotopes can build up, which will interact with the point defects resulting from the bombardment of the surface as well as with the impurities of the materials. It is important to develop an understanding of the evolution of W microstructure in such conditions and to be able to model this evolution. The task is very complex, as many elements have to be included in the model which must be all parameterized correctly. Isochronal annealings experiments are simple experiments which can help in the making of more complicated models. In this work, an object Kinetic Monte Carlo technique parameterized on ab initio calculations as been used to model He desorption in W. The He atoms and the self interstitial atoms have been found to be very mobile but they can bind quite strongly with impurities such as carbon or molybdenum atoms. The evolution of the number of defects in the Kinetic Monte Carlo simulation was found to be in good agreement with the resistivity changes observed during an He desorption experiment of above threshold He implantation in a thin wire of tungsten.

1. Introduction

One of the promising candidates for the divertor plate in International Thermonuclear Experimental Reactor (ITER) is tungsten, because of its high melting temperature, high thermal conductivity and low sputtering erosion. During its lifetime, the divertor surface will be impinged by high energy particles: helium, hydrogen isotopes and neutrons. These isotopes will interact with the point defects resulting from the displacement cascades induced by the high energy particles as well as with the impurities of the materials. These interactions will induce changes in the microstructure and thus in the mechanical properties. The overall objective of this work is to simulate radiation damage in tungsten with He production in order to predict the evolution of the microstructure and the possibility of swelling. The object kinetic Monte Carlo (OKMC) method is one of the tools which can be used to model the microstructure evolution under such conditions. However, for this modeling, the elementary physical phenomena associated with the point defects created and their interaction with the He produced have to be determined. As these phenomena take place at the atomic level, this has to be done with the help of ab initio calculations. Ab initio calculations have thus been used to parameterize an object Kinetic Monte Carlo code and simulate He desorption in W.

In a first part the OKMC model which has been used is presented. In a second part the most important parameters of the OKMC are described and compared with experimental results when possible. The OKMC code is then used in the third part to simulate an isochronal annealing experiment of He desorption in W.

2. Methodology

The OKMC code LAKIMOCA developed at EDF has been modified to take into account He.

The general features of the LAKIMOCA code have been extensively described in a previous publication [1]. Briefly, the model treats radiation produced defects (vacancies, self interstitial atoms (SIA) and their clusters) as well as foreign interstitial atoms (FIA – He in the present work) as objects with specific positions in a simulation box and with associated reaction volumes. The different events are presented in Fig. 1. Each object can migrate or emit single entities (a vacancy, a SIA, a FIA) and participate in a series of predefined reactions. The probabilities for physical transition mechanisms Γ_i, which are basically migration jumps and emission from larger defects or from traps, are calculated in terms of Arrhenius frequencies for thermally activated events,

$$\Gamma_i = \nu_i \exp\left(\frac{E_{a,i}}{k_B T}\right), \tag{1}$$

* Corresponding author. Tel.: +33 3 20 43 49 44; fax: +33 3 20 33 61 48.
E-mail address: charlotte.becquart@univ-lille1.fr (C.S. Becquart).

0022-3115/$ - see front matter © 2008 Elsevier B.V. All rights reserved.
doi:10.1016/j.jnucmat.2008.11.027

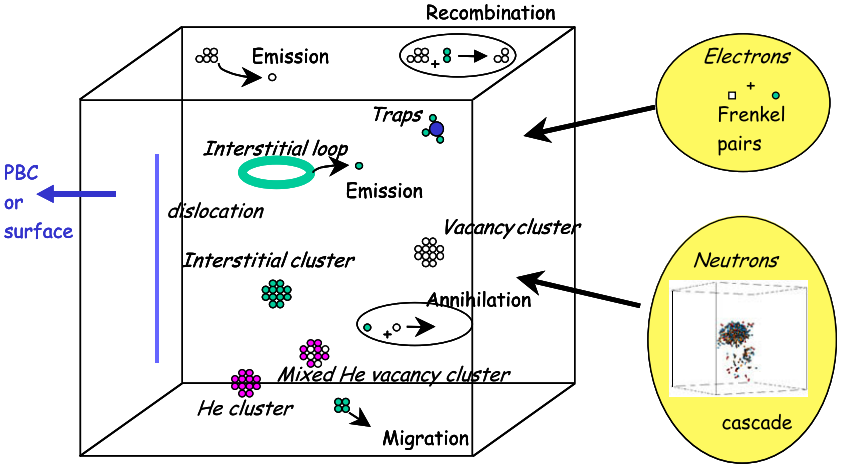

Fig. 1. Summary of the different events: migration, recombination, emission of single entities or trapping as well as electron or neutron irradiations, taking place in an object KMC simulation using the LAKIMOCA code. The dimensions of the box are $199a_0 \times 200a_0 \times 201a_0$, where a_0 is the lattice parameter of tungsten.The white spheres are the vacancies, the green ones, the SIAs; the pink ones represent the helium atoms (For interpretation of the references to colour in this figure legend, the reader is referred to the web version of this article.).

where ν_i is the attempt frequency (prefactor) for event i, $E_{a,i}$ is the corresponding activation energy, k_B is Boltzmann's constant and T is the absolute temperature. After a certain event is chosen, time is increased according to the residence time algorithm [2],

$$\Delta\tau = 1 \Big/ \sum_{i=1}^{N_e^{th}} \Gamma_i + \sum_{j=1}^{N_e^{ext}} P_j \tag{2}$$

where P_j are the probabilities of external events, such as the appearance of a cascade, of isolated Frenkel pairs produced by impinging particles, or of implanted FIAs. In addition, the model includes non-thermally activated events, such as the annihilation of a defect after encountering either a defect of opposite nature (i.e. a SIA encountering a vacancy) or a sink, as well aggregation, either by adding a point defect to a cluster or by forming a complex between a defect and a trap for it. These events occur only on the basis of geometrical considerations (overlap of reaction volumes) and do not participate in defining the progressing of time. The possibility of introducing different classes of immobile traps and sinks, characterized by specific geometrical shapes (spheres, infinite cylinders, surfaces, etc.) and suitable to mimic voids or other trapping nanofeatures, as well as dislocations and grain boundaries, is also implemented. The code is therefore equipped to mimic fairly realistic microstructures and irradiation conditions.

The choice of the parameter set is a difficult task and quite an open question. For each object, one has to define all the possible events that that object can perform, with their appropriate probabilities. The object properties are: the types of objects (e.g. a single vacancy v, a He atom, a di-vacancy, 2v, a single self interstitial atom (SIA), etc.), the forward reactions that these objects can perform with the appropriate probabilities and capture radius (e.g. the annihilation of a vacancy with a self interstitial: v + SIA $\rightarrow \varnothing$, or the formation of a di-vacancy: v + $v \rightarrow$ 2v), the backward reactions with their probabilities (e.g. the dissociation of a vacancy from a di-vacancy).

To obtain the OKMC data, ab initio calculations in the framework of the functional density and the Vienna Ab initio Simulation Package VASP [3] were used. The calculations were performed in the framework of Blöchl's projector augmented-wave (PAW) method [4] within the Generalized Gradient Approximation (GGA) of Perdew and Wang [5]. The pseudo-potentials were taken from the VASP library. The supercell approach with periodic boundary conditions (PBC) was used to simulate point defects as well as pure phases. Brillouin zone sampling was performed using the Monkhorst and Pack scheme [6]. The plane wave cut-off energy was 350 eV in order to get converged results. 54 atom supercells with 125 kpoints as well as 128 atoms with 27 kpoints were used to check the convergence of the calculations with supercell size. For clarity and because the results were converged, only the results obtained with the largest supercell size, i.e. the 128 atom supercell calculations will be presented in this article. All the structures have been relaxed by conjugate gradient, keeping the volume constant. The uncertainty on the ab initio results is 0.01 eV.

The binding energy $E_b(A_1, A_2)$ between two entities A and B is obtained as

$$E_b(A_1, A_2) = [E(A_1) + E(A_2)] - [E(A_1 + A_2) + E_{\text{Ref.}}] \tag{3}$$

where E_{Ref} is the energy of the supercell without A_1 and A_2, $E(A_j)$ is the energy of the supercell containing A_j only and $E(A_1 + A_2)$ is the energy of the supercell containing both A_1 and A_2 in interaction with each other. All the supercells contain the same number of metal sites, i.e. have the same size. Except when otherwise stated, the reference state of the binding energies presented in this work is always the energy of a supercell without any defects, i.e. a perfect crystal. With such a scheme a positive binding energy means attraction between the entities. For more than two entities, Eq. (3) can be extended as follows:

$$Eb(A_1, A_2, \ldots, A_n) = \sum_{i=1,\ldots,n} E(A_i) - [E(A_1 + A_2 + \cdots + A_n) + (n-1)E_{\text{ref}}] \tag{4}$$

with the same convention as in Eq. (3)

3. Results

3.1. Helium and vacancy clustering

The most stable interstitial configuration for He is the tetrahedral (T) site, the energy difference between the two possible interstitial sites ΔE_{T-O}, where O stands for octahedral, being equal to 0.22 eV. Furthermore, the substitutional configuration is 1.46 eV lower than the tetrahedral one.

The binding energy between interstitial He atoms [10] (Table 1), as well the binding energy of a single He atom or a single vacancy with small He-vacancy complexes have been determined. The results are shown in Table 2.

Table 1
Binding energies (eV) of one He atom to a He cluster, for He in interstitial configurations [10]. Calculations done using 128 atom supercells and 27 kpoints.

Reaction	Binding energy (eV)
He + He → 2He	1.03
He + 2He → 3He	1.36
He + 3He → 4He	1.52
He + 4He → 5He	1.64

The binding energy between two He atoms is very high, close to 1 eV, and the results in Table 1 indicate also that the formation of He bubbles without pre-existing damage is possible as was observed by Nicholson [7]. The data in Table 2 also indicate that a He atom always binds more strongly with a mixed He-vacancy cluster than a vacancy to a cluster of same composition. For larger size clusters, the data were extrapolated.

As regards the mobilities, the ab initio calculations indicate that He migration energy as an interstitial is very low, around 0.06 eV. This results is *a priori* in contradiction with the experimental values of the diffusion coefficients of He [8,9]. However it was shown in [10] that the strong tendency for He to bind with itself can explain this discrepancy with the experimental data, which are very probably migration energies of small He clusters rather than of isolated He atoms [10]. This is in perfect agreement with the results of Soltan and coworkers [11] who, in a careful study of hydrogen, deuterium, and helium implantation at 5 K with energies from 0.25 to 3 keV into thin films of 80 – 320 nm of gold and tungsten, followed by isochronally heating of the specimens up to 400 K, demonstrated that concentrations as low as 350 ppm of He suppressed He migration because of the clustering of these elements. They furthermore calculated that in the experiments of Wagner et al. [8] as well as that of Amano [9], the concentration of implanted He was 5%. They thus explain why in their own experiments, He becomes mobile at temperature below 5 K, in contradiction to the previous results [8] and [9] where mobility of ^{3}He and ^{4}He was observed only above 90 K.

The binding energy between a single vacancy and He is very high (Table 2), and thus the dissociation of such a cluster is highly improbable. However when a SIA moves close to such a complex, the W atom jumps in the vacancy and the He atom moves to a tetrahedral site and will then be able to migrate very quickly. This reaction was checked using ab initio molecular dynamics and is taken into account in our model. The possibility of He motion through the help of two vacancies, which was found to be energetically costly in Fe [12], was not investigated as the divaccancy was found not to be stable [13] and as the He · 2v complex is not very stable either (Table 2). As for the vacancy, its migration energy is 1.66 eV [13], all vacancy clusters are in principle allowed to move but their diffusion coefficients are so low, that they will not move during the isochronal annealing experiment. The He and vacancy clustering data (Tables 1 and 2) are usually represented in terms of dissociative energy (i.e. the sum of the migration energy and the binding energy) of a vacancy or an interstitial He versus the ratio of He to vacancy. This is presented in Fig. 2. The dissociation energy at the cross-over between the two curves, which shed some light on the composition of the most stable clusters as well as on their stability [14], is close to 4 eV and the He to vacancy ratio is one.

Table 2
Binding energies (eV) of He and v small clusters (xHe.yv). Calculations done using 128 atom supercells and 27 kpoints.

Reaction	He binding energy (eV)	Reaction	Vacancy binding energy (eV)
He + v → He · v	4.57	v + He → He · v	4.57
He + He · v → 2He · v	3.11	v + He · v → He · 2v	0.07
He + 2He · v → 3He · v	3.28	v + He · 2v → He · 3v	0.70
He + 3He · v → 4He · v	2.61	v + He · 3v → He · 4v	1.01
He + 4He · v → 5He · v	1.44	v + 2He → 2He · v	6.65
He + 5He · v → 6He · v	2.08	v + 2He · v → 2He · 2v	1.82
He + 2v → He · 2v	4.69	v + 2He · 2v → 2He · 3v	0.68
He + He · 2v → 2He · 2v	4.85	v + 2He · 3v → 2He · 4v	1.29
He + 2He · 3v → 3He · 3v	3.97	v + 3He → 3He · v	8.57
He + 3v → He · 3v	5.35	v + 3He · v → 3He · 2v	2.65
He + He · 3v → 2He · 3v	4.83	v + 3He · 2v → 3He · 3v	1.83
He + 2He · 3v → 3He · 3v	5.08	v + 3He · 3v → 3He · 4v	1.49
He + 4v → He · 4v	5.74	v + 4He → 4He · v	10.22
He + He · 4v → 2He · 4v	5.11		
He + 2He · 4v → 3He · 4v	5.29		
He + 3He · 4v → 4He · 4v	5.17		

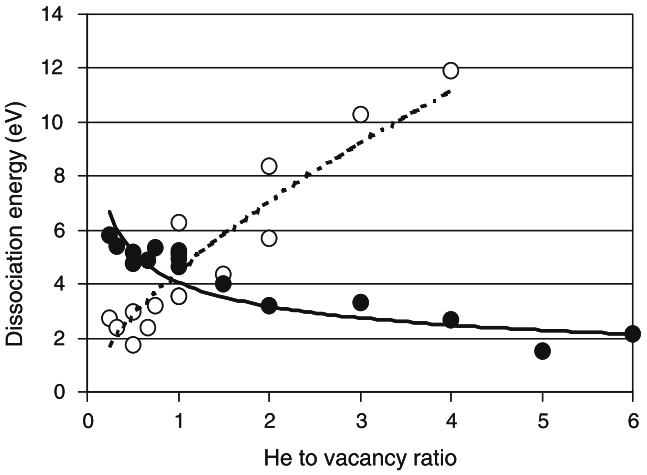

Fig. 2. Dissociation energies of a He atom or a vacancy from xHe.yv clusters as a function of He to vacancy ratio.

Table 3
Binding energies (eV) of the 'impurities' with the moving objects SIA, v and He. Calculations done using 128 atom supercells and 27 kpoints.

Species	H	He	C	Mo	Re
SIA	0.33	0.94	0.62	0.44	0.80
v	1.22	4.57	2.01	0.04	0.23
He	0.20	1.03	0.37	0.21	0.02

3.2. Influence of impurities

Impurities even in small amount play a crucial role as they can bind with the point defects and change their mobility. It was decided to investigate the possible influence of i) C as its prominent role in bcc metals is well known, ii) Mo as it is the native impurity of W, iii) Re as it can be obtained by transmutation of W. Furthermore it is commonly used as an alloying element of W to increase its re-crystallization temperature and its ductility. H which will also impinge on the surface of the divertor was also investigated. The binding energies of the vacancy, the SIA and He with these impurities are shown in Table 3. C binds very strongly with both the vacancy and the SIA which is not the case in Fe, where C binds with SIAs only when they are quite far apart [15]. H binds with both vacancies and SIAs. The binding energy with H is not negligible: 0.20 eV, and in a previous work, it was shown that H binds also very strongly with He clusters [16], in agreement with the experimental findings that He pre-irradiation of metals efficiently enhances the retention of hydrogen isotopes in the penetrated region [17,18].

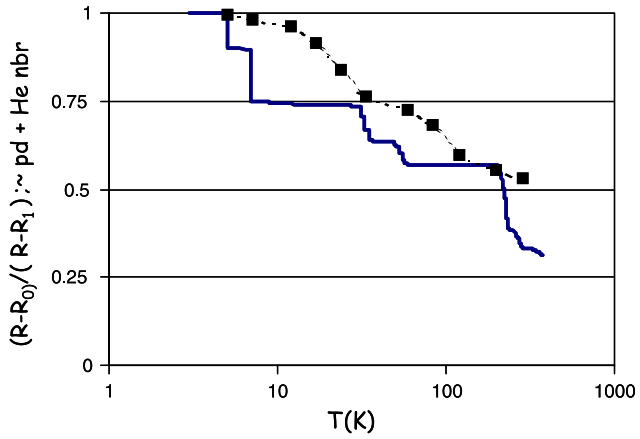

Fig. 3. Evolution of the number of defects (pd + He nbr) in the OKMC box versus annealing temperature. The black squares ($(R\text{-}R_0)/(R\text{-}R_1)$) represent the experimental resistivity recovery of Soltan et al. [11] (For interpretation of the references to colour in this figure legend, the reader is referred to the web version of this article.).

Mo does not appear to establish any interactions with vacancies, contrarily to Re whose binding energy with the vacancy is around 0.2 eV. Both Mo and Re establish strong interactions with the self interstitial atoms as can be seen from Table 3 and their most stable configuration in the vicinity of a dumbbell is as a mixed dumbbell. Mixed dumbbells in metals can be very mobile and transport solute atoms throughout the tungsten matrix. Our results indicate that Re establishes attractive interactions with both vacancies and self interstitials. These results are in very good agreement with the general finding that under irradiation, radiation induced precipitation of WRe alloys are observed [19–22] even if it needs to be comforted by the determination of the corresponding migration energies.

3.3. Self interstitial atoms and self interstitial atom cluster migration

The SIA migration energy is also quite a debated question. Indeed stage I of the isochronal annealing resistivity recovery of irradiated tungsten, which is attributed to the motion of SIAs, is composed of many peaks: 8 intrinsic recovery stages are mentioned by Dausinger [23], 6+1 by Di Carlo [24] while 5 sub-stages were observed by Coltman et al. [25] and Maury and coworkers [26]. These peaks evolve or not with dose or with the amount of impurities and the migration energy deduced by the different authors varies from 0.08 [9] to 0.54 eV [27]; More recently, Tanimoto [28] even proposed that the SIA is mobile below 1.5 K. Recent [29] molecular dynamics simulations of SIA and SIA cluster motion in tungsten using an interatomic potential derived from ab initio calculations indicate that the SIA indeed moves very quickly, with a migration energy of 0.013 eV. The SIA being a ⟨1 1 1⟩ crowdion [13,29] it moves along ⟨1 1 1⟩ directions in a 1D type motion. SIA clusters were found to be also very mobile. These results were used in our model: the SIA moves along ⟨1 1 1⟩ directions, changes direction with a rotation energy of 0.38 eV as was determined in [29]. The SIA clusters also move with the migration energy of 0.013 eV along a ⟨1 1 1⟩ direction, but they cannot change directions. The linear dependence of the diffusion coefficient with temperature demonstrated in [30] has not been included in the model.

3.4. Object kinetic monte carlo simulation of helium desorption

Using the parameters described above, a kinetic Monte Carlo simulation of He desorption was done, in the conditions of the

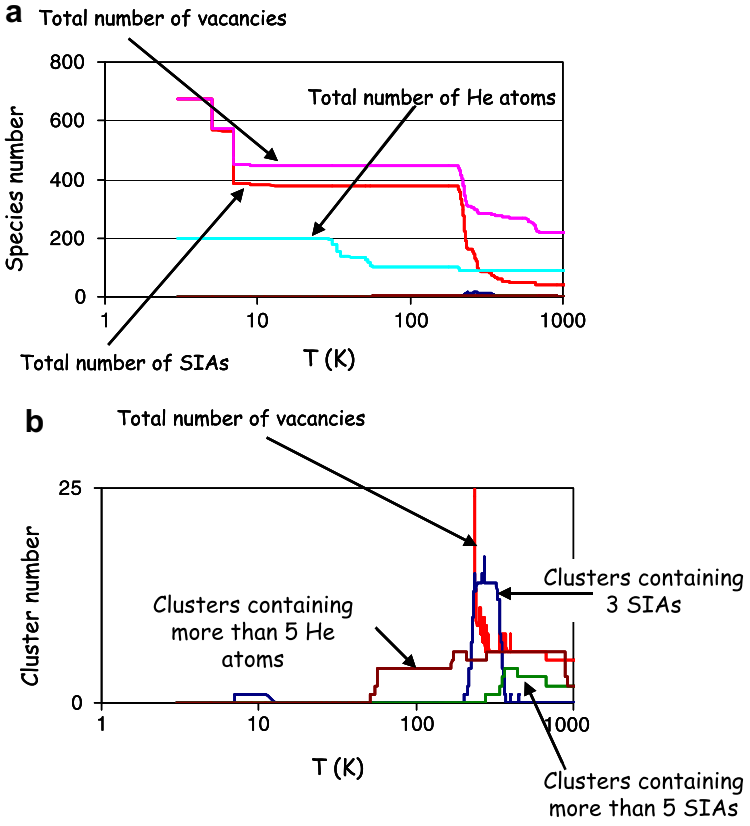

Fig. 4. Species evolution (a) total number of point defects and He atoms (b) clusters.

experiment performed by Soltan et al.[11]. In this experiment, 12 appm of 3 keV He were implanted at 5 K in thin films of W, which were subsequently isochronally annealed. According to Marlowe calculations adjusted on the cascade database produced by Seidman [31], a 3 keV He leads to the formation of 3.3 Frenkel Pairs (FP) on average. In the OKMC box, 12 ppm of He as well as the corresponding number of FP and 100 ppm of traps having the binding energy of C (Table 3) were introduced. PBC were applied in two of the three directions, simulating a thin foil of tungsten, 63 nm thick. An isochronal annealing of the whole box was then simulated by increasing the temperature by steps of 2 K every 60 s. The results are presented in Figs. 3 and 4. The decrease in the number of defects appearing before 10 K corresponds to the motion of SIAs which eliminate some vacancies, form clusters, become trapped or leave the simulation box through the surfaces. Around 25 K, the He atoms start moving, form small clusters, or bind with SIAs. A few of them bind with some of the remaining vacancies. After 200 K, the interstitials captured in the C traps are released, more mono-vacancies are thus annihilated and the number of SIA clusters increases slightly, but the overall number of defect decreases. At 500 K the microstructure consists of mono-vacancies (a little less than half the initial number), 15 vacancies in He.v clusters containing at the most 6 He atoms and SIAs clustered with He atoms (93% of the SIAs have left the simulation box) containing at the most 7 He atoms. At 1500 K, all the remaining vacancies are bound to He atoms, as He.v or 2He.v clusters; the 2% of SIAs remaining are also bound to He atoms forming slightly larger size He.SIA clusters. The overall evolution of the number of defects in the box (blue line in Fig. 3) versus temperature is quite close to the experimental data (black squares) indicating that our model reproduces correctly He desorption under these conditions. The model should of course be tested under different conditions and this will be our next objective.

4. Conclusions

The Object Kinetic Monte Carlo code LAKIMOCA was improved to take into account He. In tungsten, He atoms bind with self interstitial atoms, vacancies, impurities, hydrogen and with other He atoms. The ab initio based parameterization is capable of reproducing correctly the evolution of the defect population during an He desorption experiment in tungsten.

Acknowledgment

The authors wish to thank M. Hou for providing information about the primary damage and P. Jung for his comments. This work is supported by CEA under the collaborative contract number V 3542.001 on Fusion engineering issues, as well as CNRS under the programme interdisciplinaire énergie CHETEX. This research has been done using the CRI supercomputer of the USTL supported by the Fonds Européens de Développement Régional.

References

[1] C. Domain, C.S. Becquart, L. Malerba, J. Nucl. Mater. 335 (2004) 121.
[2] W.M. Young, E.W. Elcock, Proc. Phys. Soc. 89 (1966) 735.
[3] [a] G. Kresse, J. Hafner, Phys. Rev. B 47 (1993) 558;
[b] G. Kresse, J. Hafner, ibid. 49 (1994) 14251.
[4] G. Kresse, D. Joubert, Phys. Rev. B 59 (1999) 1758.
[5] J.P. Perdew, Y. Wang, Phys. Rev. B 45 (1991) 13244.
[6] H.J. Monkhorst, J.D. Pack, Phys. Rev. B 13 (1976) 5188.
[7] R.J.K. Nicholson, J.M. Walls, J. Nucl. Mater. 76&77 (1978) 251.
[8] A. Wagner, D.N. Seidman, Phys. Rev. Lett. 42 (1979) 515.
[9] J. Amano, D. Seidman, J. Appl. Phys. 56 (1984) 983.
[10] C.S. Becquart, C. Domain, Phys. Rev. Lett. 97 (2006) 196402.
[11] A.S. Soltan, R. Vassen, P. Jung, J. Appl. Phys. 70 (2) (1991) 793.
[12] C.C. Fu, F. Willaime, Phys. Rev. B 72 (2005) 064117.
[13] C.S. Becquart, C. Domain, Nucl. Instrum. Methods B. 255 (2007) 23.
[14] K. Morishita, R. Sugano, B.D. Wirth, T. Diaz de la Rubia, Nucl. Instrum. Methods 202 (2003) 76.
[15] C.S. Becquart, J.M. Raulot, G. Bencteux, C. Domain, M. Perez, S. Garruchet, H. Nguyen, Comput. Mater. Sci. 40 (2007) 119.
[16] C.S. Becquart, C. Domain, J. Nucl. Mater. (in press) doi:10.1016/j.jnucmat.2008.12.085.
[17] S.T. Picraux, J. Bøttiger, N. Rud, App. Phys. Lett. 28 (4) (1976) 179.
[18] S. Nagata, S. Yamamoto, K. Tokunaga, B. Tuschiya, K. Toh, T. Shikama, Nucl. Instrum. Methods, B 242 (2006) 553.
[19] J. Matolich, H. Nahm, J. Moteff, Scripta Meter. 8 (1974) 837.
[20] R.K. Williams, F.W. Wiffen, J. Bentley, J.O. Stiegler, Metal. Trans.A: 14 (1983) 655.
[21] R. Herschitz, D.N. Seidman, Acta Mater. 32 (1984) 1141.
[22] Y. Nemoto, A. Hasegawa, M. Satou, K. Abe, J. Nucl. Mater. 283–287 (2000) 1144.
[23] F. Dausinger, Phil. Mag. A 37 (1978) 819.
[24] J.A. DiCarlo, C.L. Snead, A.N. Goland, Phys. Rev. 178 (1969) 1059.
[25] R.R. Coltman, C.E. Klabunde, J.K. Redman, Phys. Rev. 156 (1967) 715.
[26] F. Maury, M. Biget, P. Vajda, A. Lucasson, P. Lucasson, Rad. Eff. 38 (1978) 53.
[27] F. Dausinger, H. Schultz, Phys. Rev. Let. 35 (1975) 1773.
[28] H. Tanimoto, M. Mzibayashi, H. Nishimura, S. Okuda, J. Phys. IV C 8 (6) (1996) C8-285.
[29] P.M. Derlet, D. Nguyen-Manh, S.L. Dudarev, Phys. Rev. B 76 (2007) 054107.
[30] S.L. Dudarev, C.R. Physique 9 (2008) 409.
[31] M. Hou, private communication.